

Optical and magneto-optical properties of MnBi film

G. Q. Di and S. Uchiyama*

Department of Electronics, Kanazawa University, Kanazawa 920, Japan

(Received 25 September 1995)

The spectral features of Kerr rotation and ellipticity of MnBi film have been found to greatly change with temperature from 85 to 475 K, and the Kerr rotation at 700 nm increases over 50%. And the complex refractive index at room temperature and the dielectric and conductivity tensors at 85, 300, and 475 K have been determined with the reflectance of an opaque film, the transmittance of a semitransparent film and the Kerr effect. There are two distinct peaks in the $\omega\sigma''_{xy}$ spectrum, corresponding well to that of Kerr rotation. By comparing those results with the reported calculations, it becomes clear that the Kerr rotations originate principally from the interband transitions of Mn $3d\downarrow$ electrons ($\hbar\omega < 2.5$ eV) and of Mn $3d\uparrow$ electrons ($\hbar\omega > 2.5$ eV). And the changes of the exchange splitting and the spin-orbit interaction strength are responsible for the strong temperature dependence of Kerr effect. Specific Faraday spectra at different temperatures have also been calculated with the above optical and dielectric constants and are much different from the reported data.

I. INTRODUCTION

Since reading information from MnBi film with a laser beam has succeeded in 1967,¹ MnBi film has intensively been investigated as a candidate of the magneto-optical (M-O) recording media. In addition to its larger perpendicular crystalline magnetic anisotropy, MnBi film also has excellent M-O effects.² The author has recently found that there are two peaks in the Kerr rotation spectrum ranging from ultraviolet to infrared: one peak reaching a maximum rotation of 1.7° is located at a wavelength of 675 nm, and a second peak with 1.4° rotation is centered at 375 nm.³ Although MnBi film has not gotten its application to the M-O recording yet because of its larger grain size which brings out a high level of media noise when the signal is read out, it still is a potential candidate for magnetic and/or M-O devices when deposition technique of film is improved in the near future. On the other hand, a recent technique can control the growth of films in the atomic scale. So it is not impossible for us to obtain new materials with designed M-O properties. In order to approach that stage, it is essential to understand the physical origins of large M-O effects, namely, to know which kind of quantum interaction is most crucial in a given solid, and how controlled atomic arrangements obtain large M-O effects at the expected wavelength. Theoretically, many calculations on M-O effects have recently been carried out with the relativistic self-consistent spin-polarization theory⁴ or the first-principles method.⁵ In order to compare with those calculations, experimental data have to be measured at low temperature, since the calculations are generally for the electronic states at 0 K and only describe the behaviors of electrons at low temperature (strictly, at 0 K). It is not enough to assess if the theoretical models are suitable by only comparing the calculations with the room-temperature data. In fact, the Kerr effect at low temperature is much different from that at room temperature.^{6,7} In addition, for discussing the origin of the M-O effect, one needs to know the off-diagonal conductivity. So it is also indispensable to obtain experimentally the reliable optical and magneto-optical constants. In the case of MnBi film, however, those

constants are sensitive to not only the film composite ratio of Mn/Bi,^{8,9} but also the surface states of films since there always remain excess manganese and/or bismuth on the film surface.¹⁰ That is why the ordinary optical constants of MnBi films were reported very differently.¹¹ It is better to measure reflectance on the opaque films but not the semitransparent films and from the substrate side but not the film surface side. For the M-O parameters, one can measure the Kerr effect instead of the Faraday effect. Because the latter, the Faraday effect, has usually to be measured on thin films and is generally enhanced by the interference waves inside films, the reported Faraday rotations of MnBi film were apparent values and hence greatly different from each other, depending on the preparations and compositions of films.¹²⁻¹⁴ And therefore, the intrinsic value of the Faraday effect of MnBi film, to our knowledge, has never been cleared.

In this paper, the author reports the optical constant of MnBi film determined from the reflectance measured on an opaque film in conjunction with the transmittance on a separate thin film, and shows the intrinsic Faraday effect derived from the optical constant and the Kerr effect in a wavelength range of 260–1500 nm. And the physical origins of the Kerr rotation are discussed from the viewpoint of electronic structure by comparing the spectra of the dielectric and conductivity tensors at low temperature with the theoretical results of the band-structure calculation by Coehoorn *et al.*⁴

II. METHODS

A. Preparations and measurements

Samples were deposited on the fused quartz substrates of 0.3 mm thick in a vacuum of 2×10^{-6} Torr with the method described elsewhere,³ and surfaces of films were all covered with a SiO protective layer of 70 nm thick for thick MnBi films before drawing from the vacuum chamber. The Kerr rotation θ_K and Kerr ellipticity η_K were measured on thick films (>170 nm) from the substrate side. Sources of light used in the measurement were Xe lamp for wavelength of 220–800 nm and W lamp for that of 800–1600 nm. Samples were set in a liquid N₂-cooled cryostat for the mea-

surement below room temperature (84–300 K) and the measurements above room temperature (300–475 K) were carried out in air. After cooling them back to room temperature, the Kerr rotations of the films used for high-temperature measurement were found to be unchanged. This implies that the films were not damaged during the high-temperature measurement and therefore the data are reliable.

For the measurement of the Kerr effect from the substrate side, the thickness of the substrate is optically much larger than the coherence length of the incident light, and therefore reflections within the substrate give rise to light waves which must be added incoherently to determine the net intensities of reflected waves. The multiple incoherent beams contribute to the measured M-O signal in proportion to their reflected intensities. So the measured Kerr rotation and ellipticity can be defined as¹⁵

$$\theta_{Km} = \frac{\sum I_n \theta_{Kn}}{\sum I_n}, \quad \eta_{Km} = \frac{\sum I_n \eta_{Kn}}{\sum I_n}, \quad (1)$$

where I_n is the intensity of n th beam. For the MnBi film, we can take, as a good approximation, only the first two beams of I_1 which is the beam intensity reflected from the front surface of the substrate and contributes no M-O signal ($\theta_1, \eta_1=0$), and I_2 reflected from the interface of the film and substrate. Then the Kerr rotation and ellipticity (observed in the substrate) can be determined as

$$\theta_K = \theta_2 = \frac{I_1 + I_2}{I_2} \theta_{Km}, \quad \eta_K = \eta_2 = \frac{I_1 + I_2}{I_2} \eta_{Km}. \quad (2)$$

B. Evaluations of optical and M-O constants

Optical constants n and k are determined by inverting normal-incidence reflectance R and transmittance T . R were measured on a thick opaque film (>170 nm) from the substrate side, and therefore influence of a possible nonmagnetic overlayer is negligible. T were measured on a separate thinner film (36 nm thick) which covered no SiO layer. It is known that the effect of such a nonmagnetic overlayer on transmittance is not so significant. The measurements for R and T were carried out at room temperature with a spectrophotometer (Hitach 340s) ranging from 190 to 2600 nm.

In finding n and k , we used the standard thin film equations¹⁶ (the effective Fresnel coefficient method) to determine the complex reflectance amplitude r and transmittance amplitude t for the electric field of a light wave incident from quartz substrate (medium 1) onto MnBi film (medium 2) normally. The back boundary of the film is an interface with air (medium 0) (for R from opaque film, this back boundary can be neglected). The total reflected and transmitted intensities are obtained as below by calculating the intensities resulting from each internal reflection in the substrate and performing an infinite sum

$$R = |r_{01}|^2 + \frac{|(1-r_{01}^2)re^{2\delta}|^2}{1-|rr_{01}e^{2\delta}|^2}, \quad (3)$$

$$T = \frac{|t_{01}te^{\delta}|^2}{1-|rr_{01}e^{2\delta}|^2}, \quad (4)$$

where

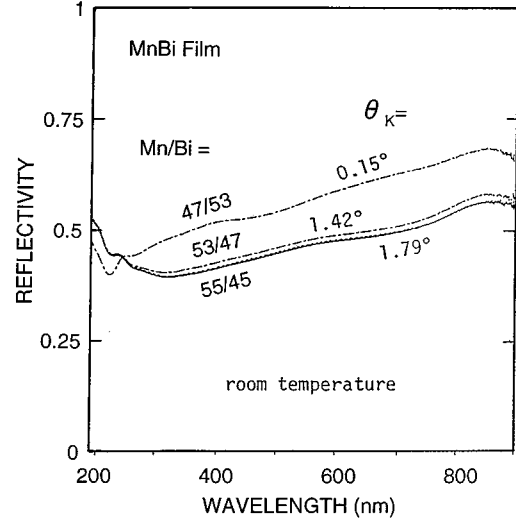


FIG. 1. Reflectivity measured on MnBi films with different compositions. Kerr rotation θ_K were measured at 700 nm.

$$r = \frac{r_{12} + r_{20}e^{ix}}{1 + r_{12}r_{20}e^{i2x}}, \quad (5)$$

$$t = \frac{t_{12}t_{20}e^{ix}}{1 + r_{12}r_{20}e^{i2x}} \quad (6)$$

and

$$x = \frac{2\pi}{\lambda} N_2 d_2, \quad \delta = -\frac{2\pi}{\lambda} k_1 d_1;$$

$$r_{ij} = \frac{n_j - n_i}{n_j + n_i}, \quad t_{ij} = \frac{2n_i}{n_j + n_i} \quad (i, j = 0, 1, 2).$$

$N_j = n_j + ik_j$ and d_j are the complex refractive index and thickness of medium, respectively. As seen in Eq. (5) r is equal to r_{12} as seen from Eq. (3) for the thick opaque film. The optical constants n_2 and k_2 of MnBi film can, therefore, be derived from R and T with Eqs. (3) and (4) using standard iteration technique. In measuring the R and T of MnBi film, one has to check if the film composition is optimum because R is also sensitive to the composition like the Kerr rotation θ_K .⁸ Figure 1 shows that R decreases with the film composition approaching to the optimum value Mn/Bi=55/45 observed in our experiment. The thin films of 36 nm thick used for measuring T in this experiment were checked to be in the optimum composition and showed a Kerr rotation as large as 1.3° at 700 nm.¹⁷

The off-diagonal element of the dielectric tensor ϵ or conductivity tensor σ were determined from the optical constants n_2 and k_2 obtained above, together with the Kerr rotation θ_K and Kerr ellipticity η_K . In this paper, we take a sign convention in which right-circular polarized (RCP) light has its electric field vector E rotating in a clockwise sense at a given point in space and the signs of Faraday rotation θ_F and Kerr rotation θ_K are positive for a clockwise rotation of the axes of the polarization ellipse, as viewed by an observer who looks in $+z$ direction when the incoming linearly polarized light from a source is traveling along the $+z$ direction

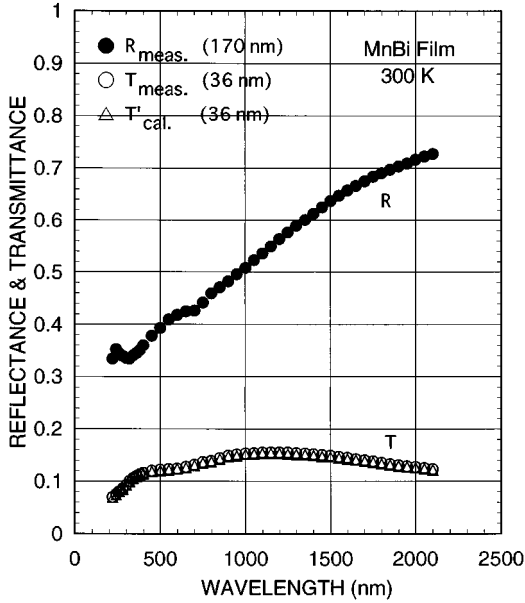


FIG. 2. Reflectance R and transmittance T used for determining the ordinary optical constants n and k . R were measured on a 170 nm thick opaque film and T on a 36 nm thick semitransparent film; T' were calculated for a system of {0.3 mm quartz substrate/36 nm MnBi film} using the determined n and k to check if the calculation for the determination of n and k is correct.

(in this definition of sign, a negative Kerr rotation and a positive Faraday rotation can be observed on Fe film in the visible spectral region). Thus we determined ε_{xy} and σ_{xy} in terms of the following equation:

$$\theta_K + i\eta_K = \frac{n_s \varepsilon_{xy}}{(n_s^2 - N_2^2) N_2} = \frac{4\pi}{\omega} \frac{i n_s \sigma_{xy}}{(n_s^2 - N_2^2) N_2}. \quad (7)$$

The intrinsic specific Faraday rotation and ellipticity can be determined from ε_{xy} with Eq. (8) or from θ_K and η_K directly with Eq. (9),

$$\theta_F + i\eta_F = -\frac{\pi}{\lambda} \frac{i\varepsilon_{xy}}{N_2} \quad (8)$$

$$= -\frac{i\pi}{\lambda} \frac{n_s^2 - N_2^2}{n_s} (\theta_K + i\eta_K), \quad (9)$$

where n_s and $N_2 = n_2 + ik_2 = (\varepsilon_{xx})^{1/2}$ are the complex refractive indexes of the substrate and the MnBi film, respectively; and $\varepsilon_{xy} = \varepsilon'_{xy} + i\varepsilon''_{xy}$ and $\sigma_{xy} = \sigma'_{xy} + i\sigma''_{xy}$.

III. RESULTS AND DISCUSSIONS

A. Ordinary optical constants

Figure 2 shows the reflectance R measured on an opaque film from the fused quartz substrate side and the transmittance T on a semitransparent film with incident light from the substrate side. In the measured wavelength region, R falls off monotonously with wavelength and does not vary steeply except below 300 nm, and T fluctuates somewhat due to the interferences of light inside the thin film. From R and T , ordinary optical constants n and k are calculated with Eqs.

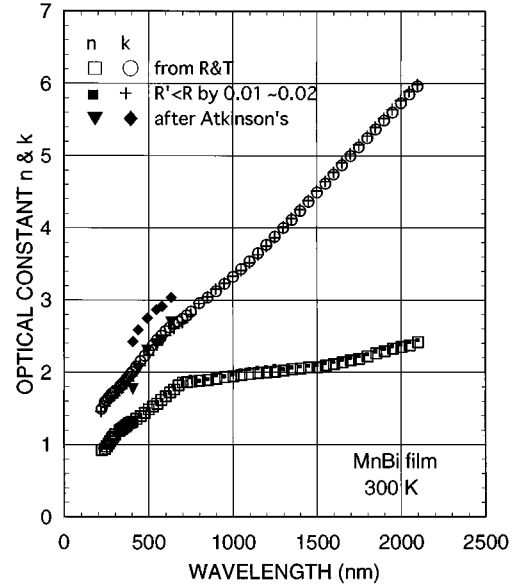


FIG. 3. Optical constant n and k determined from R and T shown in Fig. 2. ■ and + are the n and k determined supposing R' is less than R by 0.01 above 900 nm and 0.02 below 900 nm. ▼ and ◆ are the reported n and k for MnBi film (Ref. 14).

(3) and (4) as shown in Fig. 3. In the whole measured region, k is larger than n . And both n and k decreases monotonously with wavelength and exhibit some structures near 700 and 300 nm. ■ and + represent n and k , which are evaluated supposing the reflectance R was measured 0.01–0.02 smaller, i.e., R has an error of -2.5 to -5.6% . Considerable differences cannot be observed between the two sets of n and k . Similarly, if T had a ΔT of ± 0.01 (an error of 6–12%), then $\Delta n < \mp 5\%$ and $\Delta k < \mp 3\%$. So possible errors in our n and k are believed to be within $\pm 10\%$. However, our data are smaller than Atkinson's data¹³ as shown in Fig. 3 which were, to our knowledge, the most complete optical constants for MnBi film reported before our experiment. This larger difference is due to the fact that the interferences of waves inside films were neglected in their calculations of determining N and magneto-optical parameter $Q = Q' + iQ''$.¹³ We noted that Kerr effects $\Phi_{K,F}$ ($\Phi_K = \theta_K + i\eta_K$) calculated from their N , Faraday rotation F' , and ellipticity F'' with Eq. (9) are larger than our data but approximately equal to $\Phi_{K,Q}$ determined from their N and Q ($\varepsilon_{xy} = -iN^2Q$) with Eq. (7). If their N and Q are intrinsic values, $\Phi_{K,Q}$ should be much different from $\Phi_{K,F}$, because their $\Phi_{K,F}$ is an apparent value and therefore contains enhancement due to boundary effects.

Figure 4 shows frequency dependences of the real and imaginary parts of diagonal component $\varepsilon_{xx} (= \varepsilon'_{xx} + i\varepsilon''_{xx})$ of the dielectric constant at 300 K. The spectra are similar to that of transition metals, Ni for instance, rather than that of noble metals or Bi. ε'_{xx} does not pass cross zero point ($\varepsilon'_{xx} = 0$) and is always negative and less than 1, whereas ε''_{xx} falls off monotonically with increasing frequency and a faint structure which may arise from interband transitions appears near 1.8 eV. Therefore, so called plasma resonance frequency is beyond our measured region, and the large magneto-optical effect of MnBi film is not a resonancelike enhance-

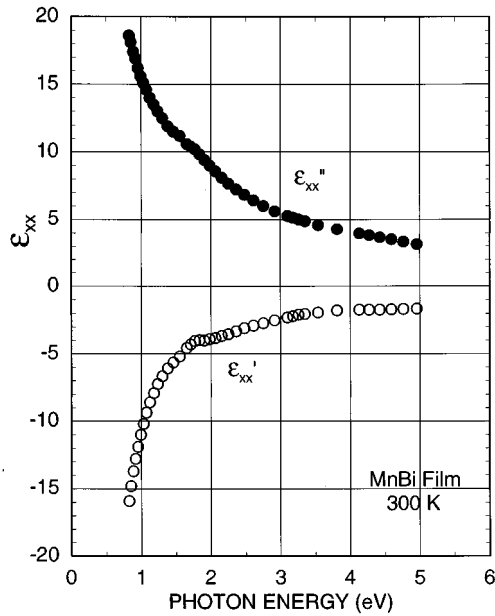


FIG. 4. Frequency dependence of the diagonal component $\epsilon_{xx} = \epsilon'_{xx} + i\epsilon''_{xx}$ of the dielectric tensor for MnBi film at room temperature.

ment in the investigated energy region, but stems mostly from the interband transitions of bound electrons.

B. Magneto-optical effects

Figure 5 shows spectra of the Kerr rotation and ellipticity of MnBi film with optimum composition at 85, 300, and 475 K. Two pronounce peaks center at 1.84 and 3.35 eV on the Kerr rotation spectra. This spectral feature is similar to those observed on Fe, Co, and Ni, all of which exhibit characteristic double peak of the Kerr rotation in the energy range of 1–5 eV.¹⁸ The Kerr rotation decreases rapidly below 1.5 eV and changes its sign at 0.91 eV at 85 K, and it is deduced to

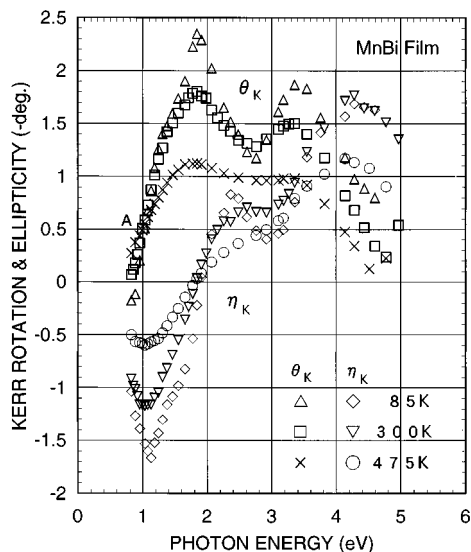


FIG. 5. Kerr rotation θ_K and Kerr ellipticity η_K spectra of MnBi film, measured at temperatures of 85, 300, and 475 K.

approach zero at 0.79 eV for 300 K and at 0.67 eV for 475 K. Corresponding to the variation of Kerr rotation, the Kerr ellipticity exhibits a minimum near 1.1 eV, a maximum near 4.3 eV, and singularity around 2.7 eV, and changes its sign near 1.8 eV. Considerable temperature variations are observed in the spectral features of both Kerr rotation and ellipticity. With increasing the temperature from 85 to 475 K, there are two other characteristics in the spectral variation. One is that the Kerr rotation stand up with different slopes at different temperatures around 1 eV, and they cross at a point A near 1 eV. The slope becomes gentle when temperature increases, and the sloping curve behaves as if it rotates around the point A as a fulcrum, resulting in a 0.25 eV displacement of the point where the Kerr rotation changes its sign on the low-energy side. The other is that the spectrum of the Kerr rotation varies in an unique way with temperature as can be seen clearly from Fig. 5. At 85 K, the two peaks of Kerr rotation are narrower and separate distinctly (the part of the valley between the two peaks is deeper). Corresponding to this valley, the Kerr ellipticity displays two clear structures around 2.7 eV. When temperature increases, the variation of Kerr rotation spectrum can be roughly divided into two parts. From 85 to 300 K, the two peaks decrease and broaden, and the part of the valley does not vary so much in its magnitude. The two spectra at 85 and 300 K still overlap one another at the part of valley. And from 300 to 475 K, the Kerr rotation spectrum translates vertically in the direction of the ordinate. Simultaneously, the two peaks become even smaller and broader, and the outline of the valley becomes obscure. The peak at 3.35 eV shifts obviously in the low-energy direction but no changes are observed on the location of the peak at 1.84 eV. Those variations will continue till the Kerr rotation disappear as the temperature approaches the Curie temperature. Unfortunately, it is technically difficult to observe those variations above 500 K because the coercive force becomes so strong that samples cannot be saturated and the crystal structure will experience a transition from the low-temperature phase to the high-temperature phase. The variations of the Kerr rotation spectrum are similar to that of Ni film above 300 K, but are much different from that of Ni film below 300 K.⁷ It has been known that changes of the spin-orbit interaction strength cause a simple translational motion of the spectrum of the Kerr rotation in the direction of the ordinate.⁵ So, the temperature dependence of the Kerr spectra of MnBi film might originate a more complicated mechanism than that of Ni film. It has also been known that an exchange splitting of the electronic structure is also essential to the Kerr rotation, in addition to the spin-orbit interaction. For ferromagnetic materials, the electronic structure changes with increasing temperature and gives rise to reductions of the exchange splitting and the saturation magnetization. This change will certainly affect the Kerr rotation. Recently Oppeneer's calculation has shown that the change in the exchange splitting causes spectral features of the Kerr rotation to change.¹⁹ It is shown that when the exchange splitting decreases, the structure of double peak tends to disappear, and the peak at higher energy moves toward the peak at lower energy and the point of $\theta_K=0$ shifts much to the low-energy side but part of the valley does not reveal a marked variation in its magnitude. Those variations are very similar to that of the Kerr rotation of MnBi film with temperature

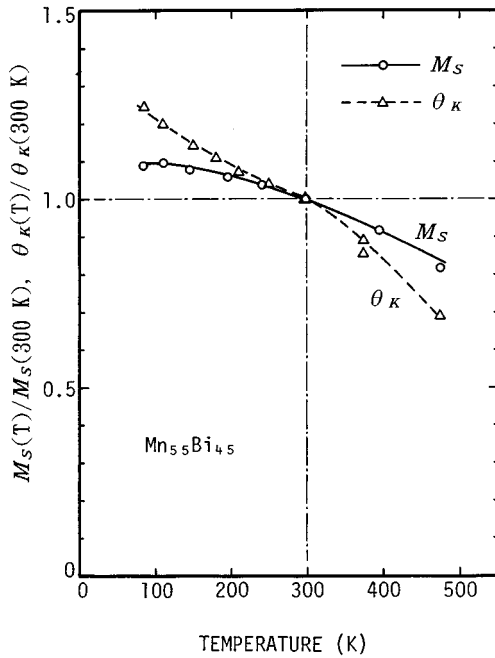


FIG. 6. Temperature dependences of the Kerr rotation θ_K at 700 nm and the saturation magnetization for a MnBi film with the optimum composition.

below 300 K shown in Fig. 5. There another calculation showed that the double spectral feature of Kerr rotation for the transition metals Fe, Co, and Ni also changes similarly with the relaxation time τ .⁵ It is well known that the τ is generally affected by all kinds of scattering mechanisms. MnBi can be expected to have a more complicated scattering mechanism than Ni, for instance, because the electrical resistance of MnBi is almost ten times larger than that of Ni and decreases by a factor of 2 as the temperature decreases from 300 to 84 K (Chen and Gondo in Ref. 2). This variation of τ will give rise to an additional temperature dependence of the Kerr rotation spectrum. Therefore, the temperature variation of the Kerr rotation spectrum of MnBi film is a synthetic effect composed of the temperature dependences of the spin-orbit interaction strength, the exchange splitting, and the relaxation time. In a practical solid, the three parameters may change simultaneously with temperature, and therefore the spectral variations cannot be simply specified. It is known that the exchange splitting increases steeply with decreasing temperature much below the Curie temperature, though the saturation magnetization changes slowly.²⁰ Oppositely, the spin-orbit interaction strength changes greatly near the Curie temperature, where the saturation magnetization quickly disappears, due to the rapid reductions in the total quantum number S and L of atoms. Considering those calculated results, it is suggested for MnBi film that the change of the exchange splitting dominates the spectral variation of the Kerr rotation below room temperature but the change in the spin-orbit interaction strength gives principal effects above room temperature. The change of the relaxation time might influence the whole temperature range.

In addition to those spectral variations, the magnitudes of the peaks of Kerr rotation reveal a strong temperature dependence. Figure 6 shows the temperature dependence of the

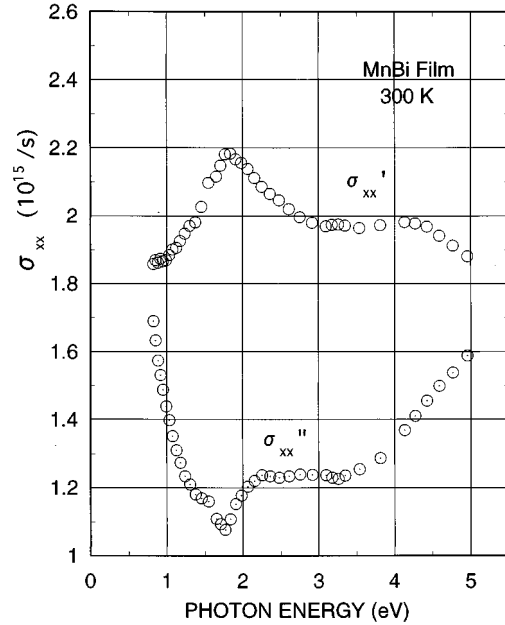


FIG. 7. Frequency dependence of the diagonal component $\sigma_{xx} = \sigma'_{xx} + i\sigma''_{xx}$ of the conductivity tensor for MnBi film at room temperature.

peak value at 1.84 eV, together with that of the saturation magnetization. When the temperature decreases from 475 to 85 K, the increment of the saturation magnetization is less than 30%, in essential agreement with the result reported by Chen *et al.*,¹³ whereas the Kerr rotation increases over 50%. This increment of the Kerr rotation is in agreement with the reported result²¹ (which was measured from the film surface with an SiO antireflection coating therefore containing the interference of light waves and showed an increment of about 20% from 300 to 85 K). It is obvious from Fig. 6 that there are no simple proportional relationships between the Kerr rotation and the saturation magnetization. This is a natural result, because the saturation magnetization is relative to the spin orientations of electrons in the $3d$ bands but the Kerr rotation depend not only on the spin orientations of electrons but also on the details of their distribution in the energy bands. And the saturation magnetization is a result contributed by all the spin-polarized electrons in unfilled shells, and the Kerr effect at given frequencies arises from only a part of electrons which occupied some energy levels and absorbed photons with the given energy. That is why the Kerr effect depends on frequency and the electronic structure can be investigated with the M-O absorption spectra.

The absorptions can be observed more clearly in the diagonal component σ_{xx} of conductivity tensor σ as shown in Fig. 7 than in ϵ_{xx} . We can see that σ'_{xx} spectrum is approximately composed of two broad absorption peaks located at 1.8 and 4 eV, respectively. The two peaks may be responsible for strong interband transitions of electrons which result in the corresponding large Kerr rotations at 1.84 and 3.35 eV, since σ'_{xx} describes the ordinary optical absorption, namely, represents a sum of absorptions for RCP and left-circular polarized (LCP) light. On the other side, the off-diagonal component σ_{xy} of conductivity tensor σ describes magneto-

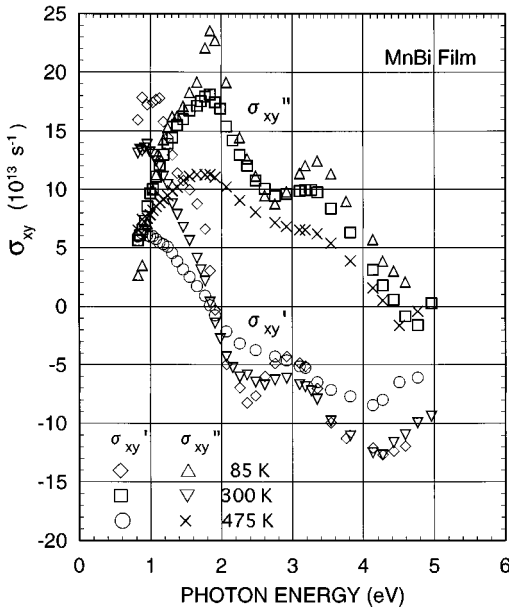


FIG. 8. Frequency dependence of the off-diagonal component $\sigma_{xy} = \sigma'_{xy} + i\sigma''_{xy}$ of the conductivity tensor for MnBi film at temperatures of 85, 300, and 475 K.

optical absorptions, and its imaginary part is proportional to the difference in the absorptions for RCP and LCP light. Figure 8 is spectra of σ_{xy} for different temperatures. In deriving those spectra at 85 and 475 K, the ordinary optical constants n and k at the room temperature are used, since the ordinary optical absorption depends very slightly on temperature²² [for example, it is $\pm 3\%$ for Ni over a temperature range of 295–770 K (Ref. 23)] and also depends slightly on the magnetization.^{24,25} In those σ_{xy} spectra, spectral structures appear more distinctly. The pronounced one is a diamagnetic structure centered at 0.9 eV, i.e., a peak of σ'_{xy} and a dispersive line shape of σ''_{xy} . Another is a paramagnetic structure located near 1.84 eV, a peak of σ''_{xy} and a dispersive of σ'_{xy} , where σ'_{xy} also changes its sign from positive to negative. In addition, another diamagnetic structure appears weakly near 2.9 eV and a paramagnetic structure at 3.35 eV. The two peaks of σ''_{xy} correspond well to the two peaks of Kerr rotation in Fig. 5.

It is known that magneto-optical effects arise generally from both interband transitions of valence electrons in valence bands and intraband transitions of free electrons in conduction bands. In infrared and visual regions, the contribution of free electrons to σ''_{xy} is proportional to $(\omega\tau)^{-1}$.^{26,27} In $\omega\sigma''_{xy}$ spectrum shown in Fig. 9, hence, the free electron's contributions will be a constant proportional to $1/\tau$. So, the structure of double peak in $\omega\sigma''_{xy}$ represent the magneto-optical Kerr absorption due to the interband transitions of valence electrons between occupied and unoccupied states, and therefore reflect the density of state (DOS) distribution of electrons near the Fermi level, since $\omega\sigma''_{xy}$ scales both the joint density of states and the joint spin polarization. According to the self-consistent spin-polarized band-structure calculation,⁴ the Mn atoms in MnBi have an effective $3d^{5.5}$ configuration, being responsible for a magnetic moment of $3.6\mu_B$. The Mn $3d$ band is split about 3.5 eV by exchange

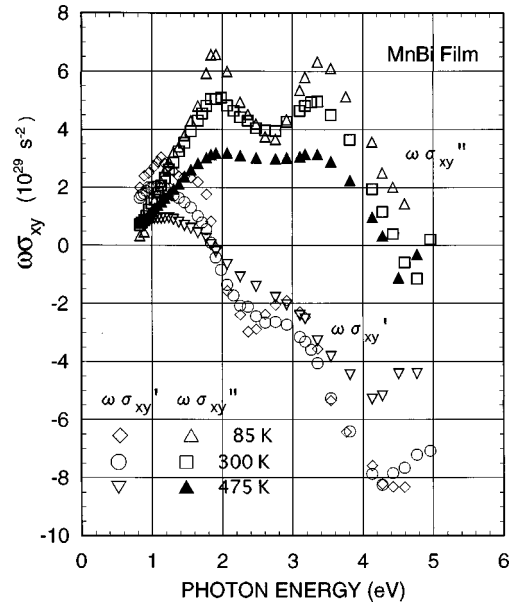


FIG. 9. $\omega\sigma''_{xy}$ spectra of MnBi film at 85, 300, and 475 K, respectively.

interaction. Its density of states for the majority-spin direction (\uparrow) $3d$ electrons shows a peak around 2.5 eV below the Fermi level, and for the minority-spin direction (\downarrow) $3d$ electrons, a main peak situates at 0.5 eV above the Fermi level and a weak peak is observed near -1 eV. As a whole, the number of the minority-spin electrons is larger than that of the majority-spin electrons near the Fermi surface. The Bi $6p$ band strongly hybrid with the Mn $3d$ band both below and above the Fermi level. The electrons in the states below the Fermi level will be excited up to the states above the Fermi level after absorbing radiation energy. The initial and final states for the possible transitions at a symmetry point Γ of the first Brillouin zone for the hexagonal lattice of MnBi was given theoretically by Coehoorn and de Groot^{4,28} as shown in Fig. 10. For understanding easily, only the main states are shown in this figure. The abscissa is the strength of the spin-orbit interaction, whose magnitude has not been clear yet for the MnBi compound. The ordinate is the electron energy. All initial states (5^+ and 1^+) for the interband transitions have positive parity, and the final states that are magneto-optically active are 6^- and 4^- states which are split by the exchange interaction and show a large spin-orbit interaction. The 6^- states have strongly mixed majority-minority character. In our Kerr measurement, the magnetic moment and the incidence of the polarized light are all along the c -axis ([001] direction of NiAs-type structure). According to Coehoorn, the possible interband transitions are denoted with arrows in Fig. 10. It is obvious that the contributions to $\omega\sigma''_{xy}$ or the Kerr effect in region $\hbar\omega < 2.5$ eV are essentially from the transitions of $3d\downarrow$ electrons at 5^+ and 1^+ states, marked with dashed arrows. Therefore the difference between the oscillator strengths for the right- and left-circular polarized light is large because of the absence of the up-spin electrons, and explains the paramagnetic structure appearing in σ_{xy} or $\omega\sigma_{xy}$ and therefore the large Kerr rotation around 1.84 eV. Similarly, the peak of $\omega\sigma''_{xy}$ or Kerr rotation at 3.35 eV arises from the following interband transitions:

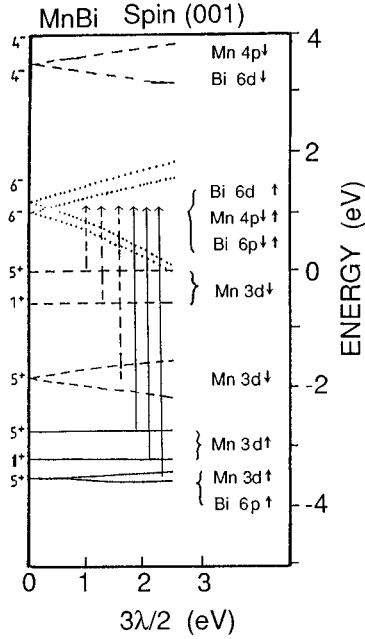


FIG. 10. Band structure at Γ as a function of the spin-orbit parameter λ for the case of spins along the c axis. —, states which are predominantly of majority-spin character; -----, states which are predominantly of minority-spin character; ·····, states which have a strongly mixed majority-minority spin character (Ref. 4).

$$\text{Mn } 3d\uparrow(5^+, 1^+) \rightarrow \text{Mn } 4p\uparrow(6^-), \text{Bi } 6p\uparrow(6^-),$$

$$\text{Bi } 6p\uparrow(5^+) \rightarrow \text{Bi } 6d\uparrow(6^-).$$

We noticed that the peaks of $\omega\sigma''_{xy}$ (paramagnetic structure) at 1.84 and 3.35 eV are corresponding well to the electronic transitions from 5^+ states which are split by the spin-orbit interaction near -1.9 and -3.6 eV in Fig. 10. In addition, the final state 6^- is split and goes down to the Fermi level because of the large spin-orbit interaction. This large splitting might be the origin of the diamagnetic structure at 0.9 eV (the transitions of electrons occupied at 5^+ and 1^+ located at -0.1 and -0.5 eV) and at 2.9 eV (the transitions from 5^+ and 1^+ located at -2.7 and -3.3 eV) of the spectra of σ_{xy} or $\omega\sigma_{xy}$. When temperature increases, there will be two variations in the electronic structure. One is that electrons at lower-energy levels are excited thermally to higher-energy levels, resulting in variations in the absorption strength for RCP and LCP light. The other is that majority electrons change their spin direction and become minority electrons, which is represented by a decrease of the saturation magnetization. Consequently, the spin-orbit interaction strength and the exchange splitting change corresponding to the two variations and result in great variations in the spectral feature of Kerr rotation. We also noticed that the two peaks of $\omega\sigma''_{xy}$ almost have the same magnitude. It might reveal a fact that the M-O absorption strength at 1.84 eV is equal to that at 3.35 eV, and this feature is less dependent on temperature.

For further understanding the details of the origin of the large Kerr effect and its temperature dependence, it would be helpful to perform an *ab initio* calculation of the Kerr rota-

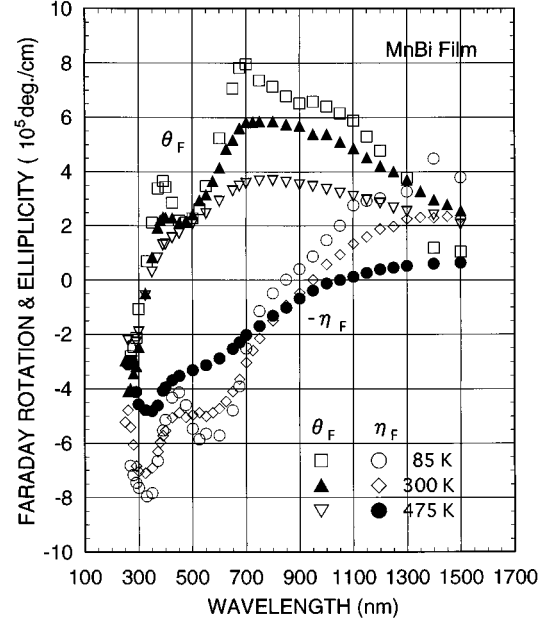


FIG. 11. Specific magneto-optical Faraday rotation θ_F and Faraday ellipticity η_F spectra of MnBi film at 85, 300, and 475 K, calculated with Eq. (8).

tion spectrum of MnBi film. By fitting the calculations to the experimental data, the magnitudes and temperature dependences of both the spin-orbit interaction strength and the exchange splitting can be traced.

On the other side, Faraday rotation spectra of the low-temperature phase MnBi film had been reported much differently in 1970's.^{24,12} The differences are due to the different preparations of films since those as-measured data were mixed with the boundary effects and the influence of the mica substrate. We are able to calculate intrinsic values of the magneto-optical Faraday effect of MnBi film with Eq. (8). Figure 11 is the calculated results for the Faraday rotation and ellipticity spectra at different temperatures, where we assumed again the ordinary optical constants are approximately independent on temperature and therefore used n and k at room temperature. It has to be noted that those data are the results of waves traveling in the positive z direction inside MnBi for 1 cm long, and without boundary effects. At 85 K, there are three main structures originating from inter-band transitions in the Faraday rotation spectrum, which center at 350, 700, and 1000 nm, respectively. The maximum peak is at 700 nm and reaches 7.96×10^5 deg/cm, and θ_F changes its sign at 310 nm. Corresponding to θ_F , Faraday ellipticity η_F get a peak of 7.95×10^5 deg/cm at 330 nm and another peak of 5.85×10^5 deg/cm at 525 nm, and changes its sign at 850 nm. With increasing temperature from 85 to 475 K, two peaks of θ_F at 350 and 1000 nm seem to disappear, and the maximum peak at 700 nm reduces to 3.68×10^5 deg/cm and shifts its location to 800 nm. Correspondingly, the peak of η_F at 525 nm disappears and that at 330 nm reduces to 4.8×10^5 deg/cm, and the point of $\eta_F=0$ largely shifts from 850 to 1050 nm.

Practically, the Faraday effect is usually measured on semitransparent thin films and the results, hence, will be much different from those in Fig. 11 due to the boundary

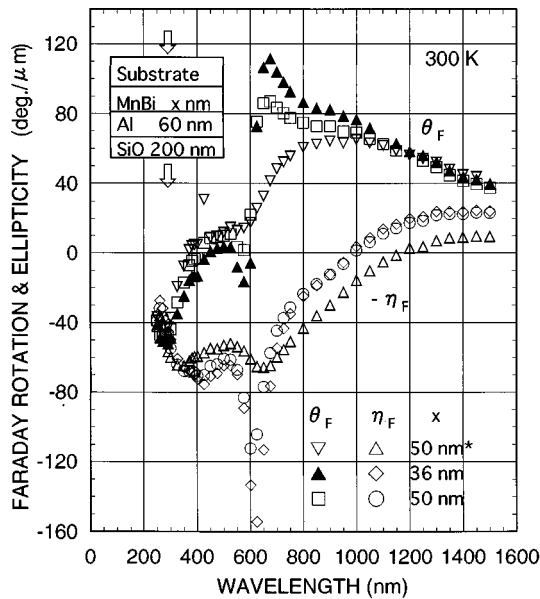


FIG. 12. Faraday rotation and ellipticity spectra, which were simulated for some practical films at room temperature with taking the bound effect into account. ∇ and \triangle are for a structure of {substrate/MnBi 50 nm/SiO 200 nm}; the other are for that of {substrate/MnBi x nm/Al 60 nm/SiO 200 nm} with $x=36$ (\blacktriangle and \diamond) and $x=50$ (\square and \circ).

effects (or multiple interferences of waves), depending on the details of films. Figure 12 displays some stimulant results of MnBi films with two types of practical structures. The Faraday rotations and ellipticities are calculated from the complex transmittance amplitudes in Eq. (6) for RCP and LCP light with Connell's equation,²⁹ supposing the light transmits through films from the substrate side. The case of $x=50$ nm* is for the structure of {quartz substrate 0.3 mm/MnBi 50 nm/SiO 200 nm}; the others are for that of {quartz substrate 0.3 mm/MnBi x nm/Al 60 nm/SiO 200 nm ($x=36, 50$ nm)}. The latter are a typical type of structure for MnBi film, being similar, for instance, to those in Refs. 11 and 12, in which there is an overlayer composed of excess Mn, Bi, and/or their oxidations on the surface of MnBi, and a protective layer of SiO on the top of film. Here we used an Al layer as a substitution of the overlayer since n and k of the overlayer are unknown. From Fig. 12, it is clear that resonances occur near 600 nm and the Faraday effect can be greatly enhanced if there is a protective layer and an overlayer. So, the Faraday effect strongly depends on the method of preparation and the structures of films even if the composition of MnBi film is optimum. That is why it was reported much differently by different researchers.

IV. SUMMARY

Ordinary optical constants n and k of MnBi film at room temperature in a wavelength range of 220–2100 nm have been determined from the reflectance measured on an opaque thick film and the transmittance on a semitransparent thin

film. And the spectra of dielectric and conductivity tensor have also been derived from the n , k , and Kerr effect. The frequency dependence of diagonal component ϵ_{xx} of the dielectric constant at 300 K is similar to that of magnetic 3d-transition metals. Because the plasma resonance frequency does not appear in the measured region, the large magneto-optical effect of MnBi film is not a resonancelike enhancement. In $\omega\sigma''_{xy}$ spectrum at 85 K, there are two distinct peaks at 1.84 and 3.35 eV, well corresponding to the two peaks of Kerr rotation. The spectral features of the Kerr rotation and Kerr ellipticity greatly change with the temperature from 475 to 85 K. And the Kerr rotation at 700 nm increases over 50% whereas the increment of the saturation magnetization is less than 30%, suggesting that the Kerr effect and the magnetization depend on the electronic structure in different ways and therefore show different temperature dependences.

By comparing the spectra of the dielectric and conductivity tensors with the reported calculations, it is clear that the Kerr rotations of MnBi film are principally from the interband transitions of Mn 3d minority electrons for $\hbar\omega < 2.5$ eV and of Mn 3d majority electrons for $\hbar\omega > 2.5$ eV. Because the electronic structure changes with temperature, the exchange splitting and the spin-orbit interaction strength depend on temperature, which are considered to be responsible for the strong temperature dependence of the Kerr effect. Taking Oppeneer's calculations into account, it is suggested that the change in the exchange splitting dominates the changes of the spectral feature of the Kerr rotation below room temperature but that of the spin-orbit interaction strength contributes great effects to the spectral change above room temperature, since the exchange splitting increases steeply with decreasing temperature much below the Curie temperature and the spin-orbit interaction strength changes greatly near the Curie temperature where the saturation magnetization quickly disappears due to the rapid reductions in the total quantum number S and L of atoms. The variation of the relaxation time will give the Kerr effect an additional temperature dependence.

The intrinsic magneto-optical Faraday spectra at different temperatures have been calculated with the ordinary optical constants and the off-diagonal component of dielectric tensor, and found to be different from the reported result. At 85 K, there are three main structures of the Faraday rotation spectrum, which center at 350, 700, and 1000 nm, respectively. The maximum peak is at 700 nm and reaches 7.96×10^5 deg/cm, and θ_F changes its sign at 310 nm. With increasing temperature from 85 to 475 K, two peaks of θ_F at 350 and 1000 nm tend to disappear, and the maximum peak at 700 nm reduces to 3.68×10^5 deg/cm.

For the further understanding of the Kerr effect of MnBi film, it is significant to carry out an *ab initio* calculation and to fit it to the experimental results. Thus the spin-orbit interaction strength and the exchange splitting and their temperature dependences could be understood.

ACKNOWLEDGMENTS

The author would like to thank S. Iwata, K. Sato, and S. Tsunashima.

- * Also at Department of Information and Communication, Aichi Institute of Technology, Toyota 470-03, Japan.
- ¹D. Chen, J. F. Ready, and E. G. Bernal, *J. Appl. Phys.* **39**, 3916 (1968).
- ²The Kerr rotation θ_K of MnBi film was reported to be 0.9° by D. Chen and Y. Gondo in *J. Appl. Phys.* **35**, 1024 (1964); 2° by R. L. Aagard, F. M. Schimit, W. Walters, and D. Chen, *IEEE Trans. Magn.* **MAG-7**, 380 (1971); 0.7 and 1.8° by K. Egashira and T. Yamada, *J. Appl. Phys.* **45**, 3643 (1974); 1.5° by M. Masuda, I. Izawa, S. Yoshino, S. Shiomi, and S. Uchiyama, *Jpn. J. Appl. Phys.* **26**, 707 (1987).
- ³G. Q. Di, S. Iwata, S. Tsunashima, and S. Uchiyama, *J. Magn. Soc. Jpn.* **15**, 191 (1991); *J. Magn. Mater.* **104-107**, 1023 (1992).
- ⁴R. Coehoorn and R. A. de Groot, *J. Phys. F* **15**, 2135 (1985).
- ⁵P. M. Oppeneer, T. Maurer, J. Sticht, and J. Kubler, *Phys. Rev. B* **45**, 10 924 (1992); P. M. Oppeneer, J. Sticht, T. Maurer, and J. Kubler, *Z. Phys. B* **88**, 309 (1992).
- ⁶G. Q. Di, S. Iwata, S. Tsunashima, and S. Uchiyama, *J. Magn. Soc. Jpn.* **16**, 113 (1992). Also see *IEEE Trans. J. Magn. Jpn.* **7**, 792 (1992).
- ⁷G. Q. Di and S. Uchiyama, *J. Appl. Phys.* **75**, 4270 (1994).
- ⁸K. Egashira and T. Yamada, *J. Appl. Phys.* **45**, 3643 (1974). In this paper, the maximum Kerr rotation was only 0.7° , and far less than 1.8° reported by the same group in *IEEE Trans. Magn.* **MAG-10**, 587 (1974).
- ⁹G. Q. Di, S. Iwata, and S. Uchiyama, *J. Magn. Mater.* **131**, 242 (1994).
- ¹⁰Y. Iwama, U. Mizutani, and F. B. Humphrey, *IEEE Trans. Magn.* **MAG-8**, 448 (1972).
- ¹¹R. Atkinson, *Thin Solid Films* **37**, 195 (1976), and references therein.
- ¹²E. Feldtkeller, *IEEE Trans. Magn.* **MAG-8**, 481 (1972).
- ¹³D. Chen, G. N. Otto, and F. M. Schimit, *IEEE Trans. Magn.* **MAG-9**, 66 (1973).
- ¹⁴R. Atkinson and P. H. Lissberger, *Int. J. Magn.* **6**, 227 (1974).
- ¹⁵W. A. Challener and S. L. Grove, *Appl. Opt.* **29**, 3040 (1990).
- ¹⁶O. S. Heavens, *Optical Properties of Thin Solid Films* (Dover, New York, 1965).
- ¹⁷Guo-Qing Di, Doctoral thesis, Nagoya University, 1992.
- ¹⁸G. S. Krinchik and V. A. Arlem'eV, *Sov. Phys. JETP* **26**, 1080 (1968).
- ¹⁹P. M. Oppeneer and V. N. Antonov, in *Spin-orbit Influenced Spectroscopies of Magnetic Solids*, edited by H. Ebert and G. Schutz (Springer, Heidelberg, in press).
- ²⁰D. K. Misemer, *J. Magn. Mater.* **72**, 267 (1988).
- ²¹J. X. Shen, R. D. Kirby, and D. J. Sellmyer, *J. Appl. Phys.* **69**, 5984 (1991).
- ²²W. Jung, *J. Appl. Phys.* **36**, 2422 (1965).
- ²³M. Shiga and G. P. Pelles, *J. Phys. C* **2**, 1487 (1969).
- ²⁴D. Chen and R. L. Aagard, *J. Appl. Phys.* **41**, 2530 (1970).
- ²⁵G. Q. Di (unpublished). There are almost no differences in reflectance from low-temperature phase MnBi film and quenched high-temperature phase MnBi film, although their magnetizations are much different.
- ²⁶J. L. Erskine and E. A. Stern, *Phys. Rev. B* **8**, 1239 (1973).
- ²⁷W. Reim, O. E. Husser, J. Schoenes, E. Kaldis, P. Wachter, and K. Seiler, *J. Appl. Phys.* **55**, 2155 (1984).
- ²⁸R. Coehoorn, C. Haas, and R. A. de Groot, *Phys. Rev. B* **31**, 1980 (1985).
- ²⁹G. A. N. Connell, *Appl. Opt.* **22**, 3155 (1983).